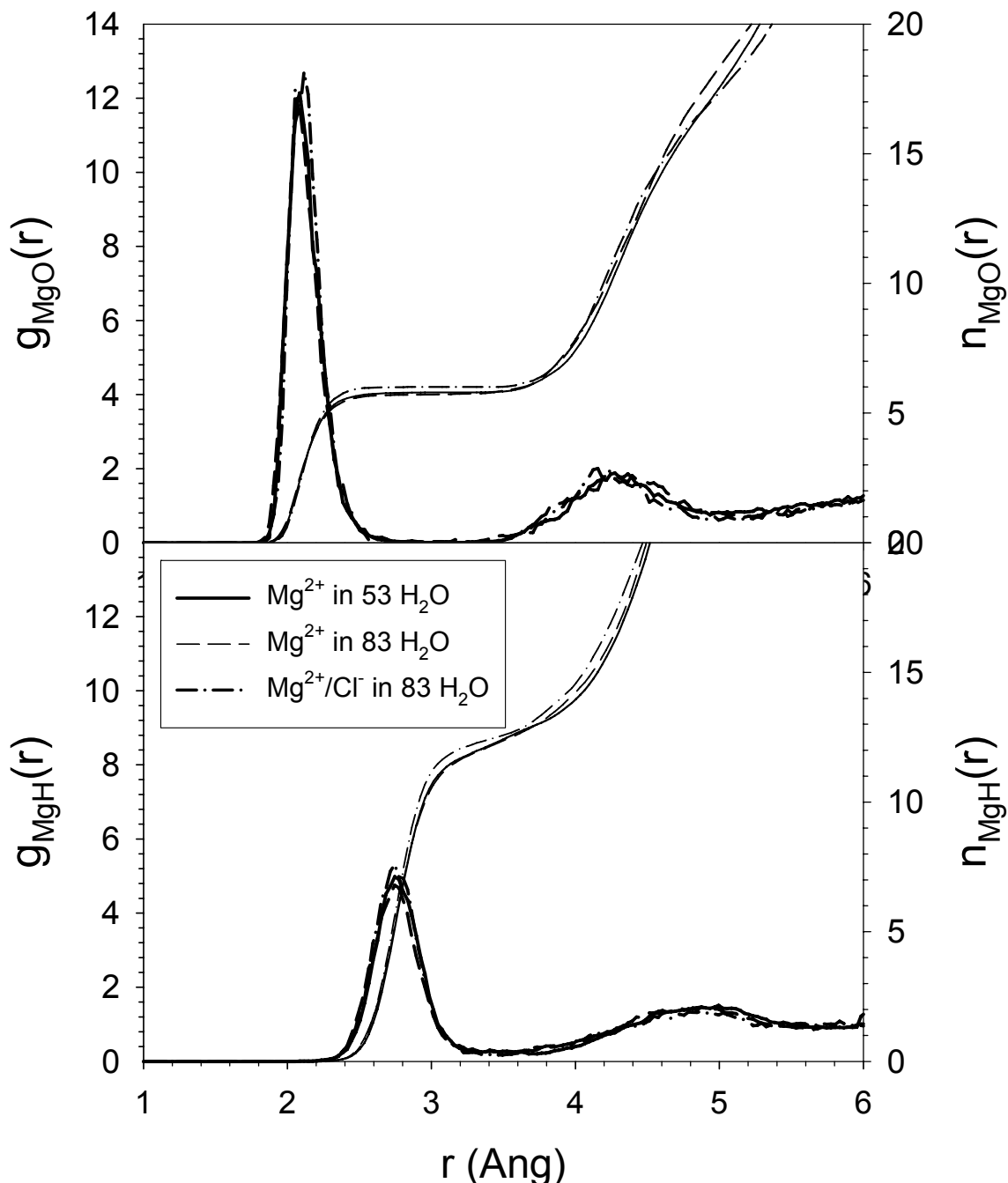


**Table SI-1.** Optimised structures (distances in Å and angles in degrees), hydration energies of the first solvation shell,  $\Delta E$ , and successive water binding energies,  $\Delta E_{\text{inc}}$ , (in kcal mol<sup>-1</sup>) of the  $\text{Mg}(\text{H}_2\text{O})_n^{2+}$  clusters computed using the PBE/US-PW and PBE/DNP methods <sup>a)</sup>.  $\Delta E = E[\text{Mg}(\text{H}_2\text{O})_n^{2+}] - E[\text{Mg}^{2+}] - nE[\text{H}_2\text{O}]$ ;  $\Delta E_{\text{inc}} = E[\text{Mg}(\text{H}_2\text{O})_{n+1}^{2+}] - E[\text{Mg}(\text{H}_2\text{O})_n^{2+}] - E[\text{H}_2\text{O}]$ . In all PWSCF calculations, cutoffs for the smooth part of the wavefunctions and the augmented density were set to 30 and 200 Ry.

	$r(\text{Mg}-\text{O})$		$r(\text{O}-\text{H})$		$\theta(\text{H}-\text{O}-\text{H})$		$\Delta E$		$\Delta E_{\text{inc}}$	
	DNP	PW	DNP	PW	DNP	PW	DNP	PW	DNP	PW
$\text{H}_2\text{O}$			0.97	0.99	104.0	104.5				
$\text{Mg}(\text{H}_2\text{O})^{2+}$	1.94	1.92	0.99	1.00	105.7	106.1	-81.7	-85.3	-81.7	-85.3
$\text{Mg}(\text{H}_2\text{O})_2^{2+}$	1.96	1.94	0.99	1.00	105.5	106.1	-153.6	-158.5	-72.0	-73.2
$\text{Mg}(\text{H}_2\text{O})_3^{2+}$	1.99	1.98	0.98	1.00	105.4	105.8	-212.4	-217.3	-58.7	-58.8
$\text{Mg}(\text{H}_2\text{O})_4^{2+}$	2.02	2.01	0.98	0.99	105.4	105.7	-259.8	-263.6	-47.4	-46.3
$\text{Mg}(\text{H}_2\text{O})_5^{2+}$	2.07	2.07	0.98	0.99	105.7	106.3	-291.9	-294.1	-32.1	-30.5
$\text{Mg}(\text{H}_2\text{O})_6^{2+}$	2.11	2.11	0.98	0.99	106.1	106.4	-321.1	-321.9	-29.2	-27.8

<sup>a)</sup> All-electron calculation using the DMol<sup>3</sup> code (Delley, B. J. Chem. Phys. 1990, 92, 508; Delley, B. J. Chem. Phys. 2000, 113, 7756), the PBE density functional and the double-numeric-polarised (DNP) basis sets on all atoms method.



**Figure SI.1.** Mg–O and Mg–H radial distribution functions,  $g(r)$ , and running coordination number,  $n(r)$ , obtained from the CP-MD simulations of  $\text{Mg}^{2+}$  in 53 H<sub>2</sub>O,  $\text{Mg}^{2+}$  in 83 H<sub>2</sub>O and  $\text{Mg}^{2+}/\text{Cl}^-$  in 82 H<sub>2</sub>O.

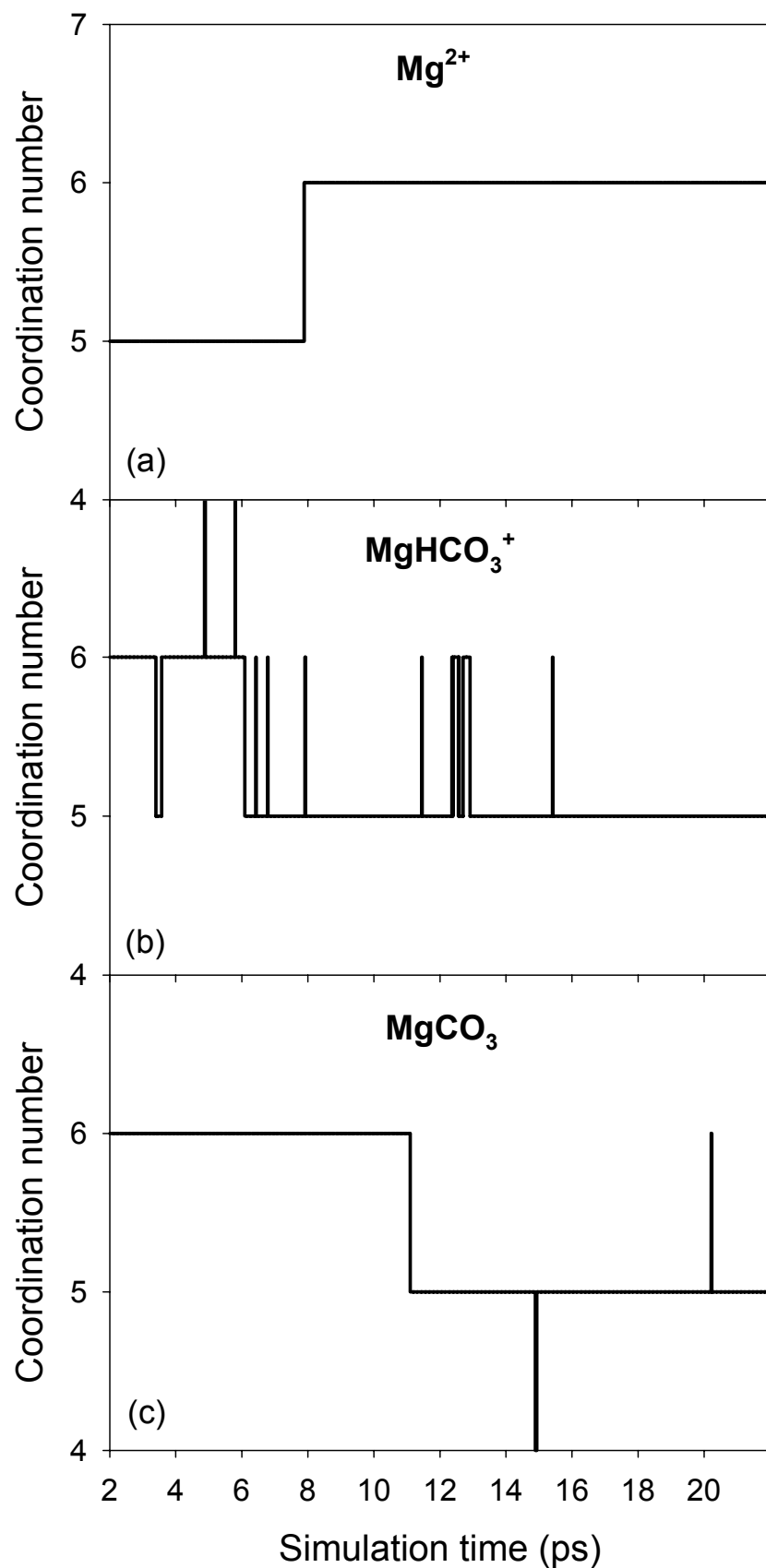


**Figure SI.2.** Time dependence of the first-shell coordination number of the magnesium atom obtained from the CP-MD simulations of (a)  $\text{Mg}^{2+}$ , (b)  $\text{MgHCO}_3^+$  and (c)  $\text{MgCO}_3$  in water.

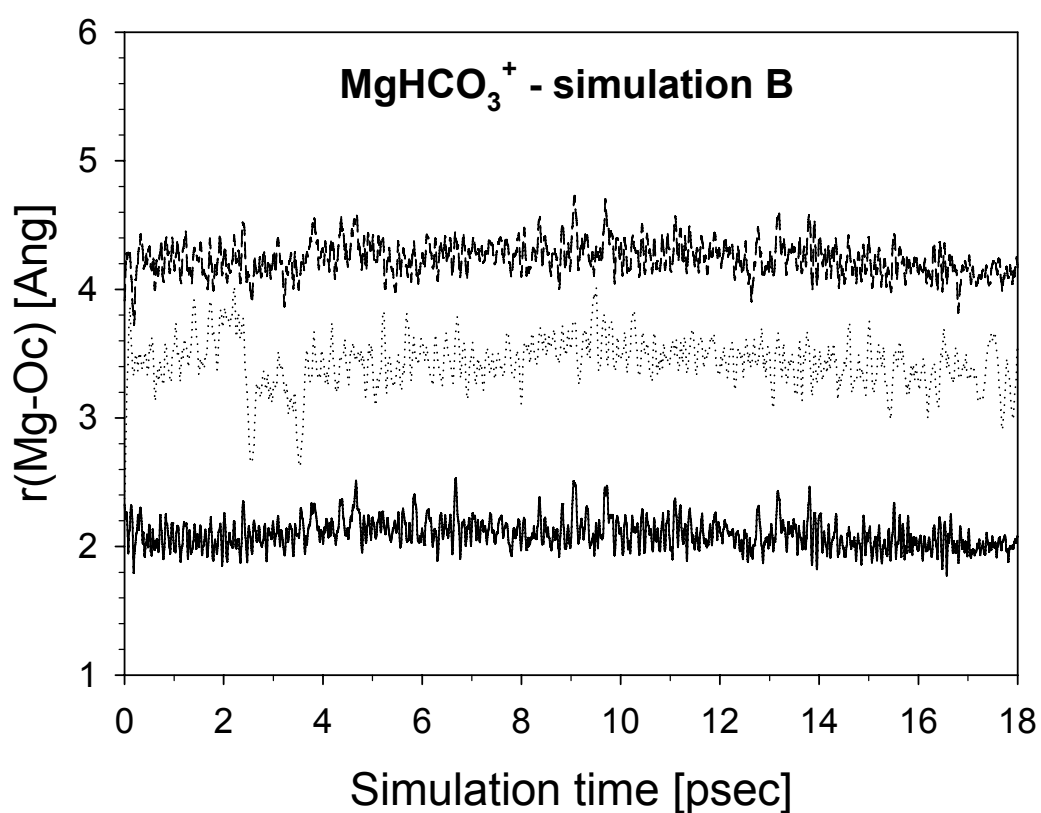
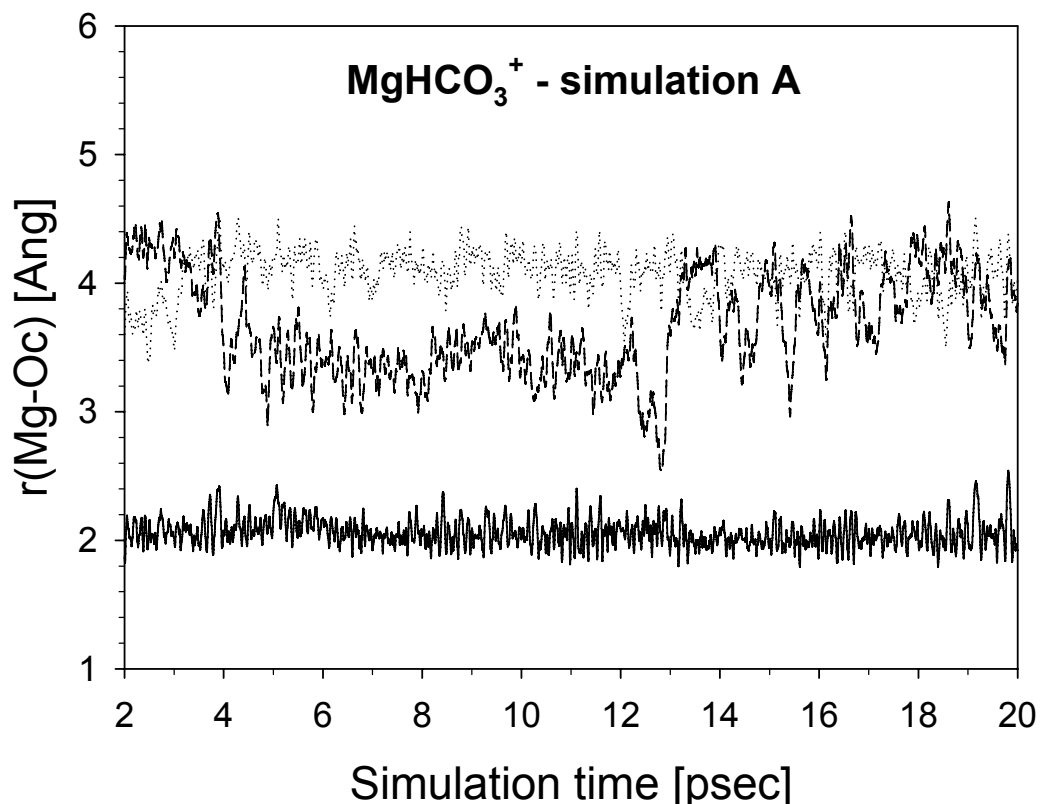


**Figure SI.3.** Time evolution of Mg–O distances for the oxygen atoms of the bi-carbonate ion. In Simulation A the initial coordination of HCO<sub>3</sub><sup>−</sup> to the magnesium

was mono-dentate ( $\eta^1$ ); in simulation **B** the initial coordination of  $\text{HCO}_3^-$  to the magnesium was bi-dentate ( $\eta^2$ ).

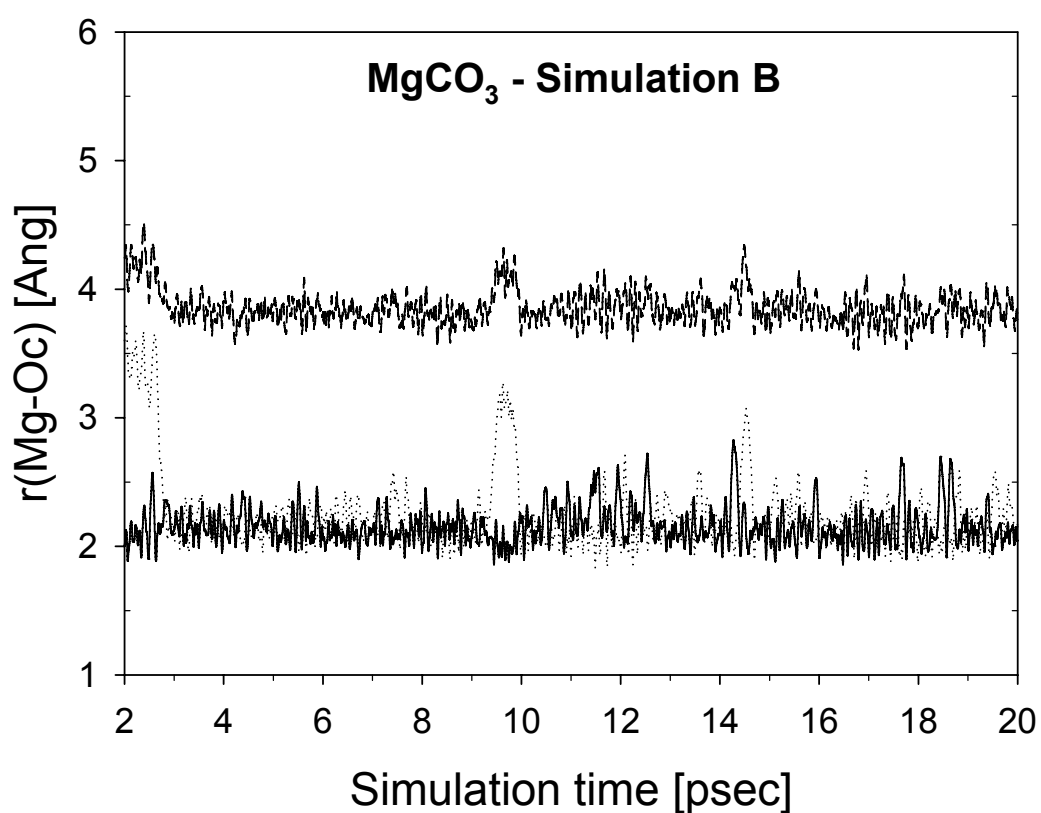
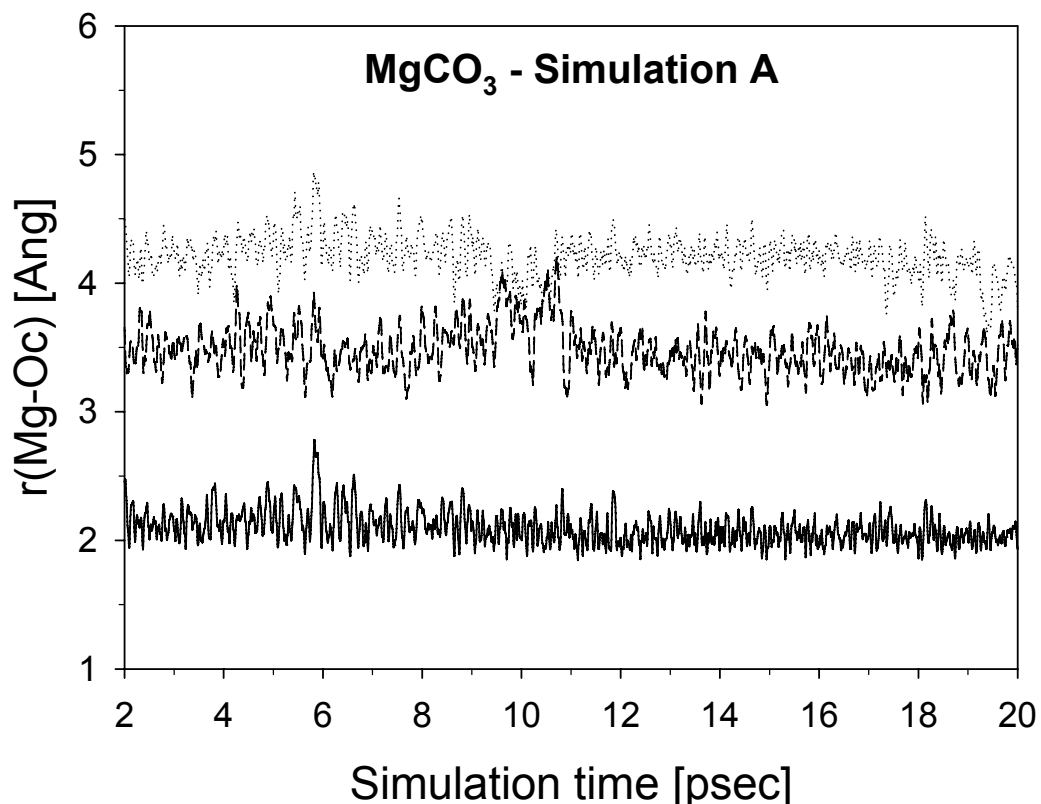


**Figure SI.4.** Time evolution of Mg–O distances for the oxygen atoms of the bi-carbonate ion. In Simulation A the initial coordination of HCO<sub>3</sub><sup>−</sup> to the magnesium

was mono-dentate ( $\eta^1$ ); in simulation **B** the initial coordination of  $\text{HCO}_3^-$  to the magnesium was bi-dentate ( $\eta^2$ ).

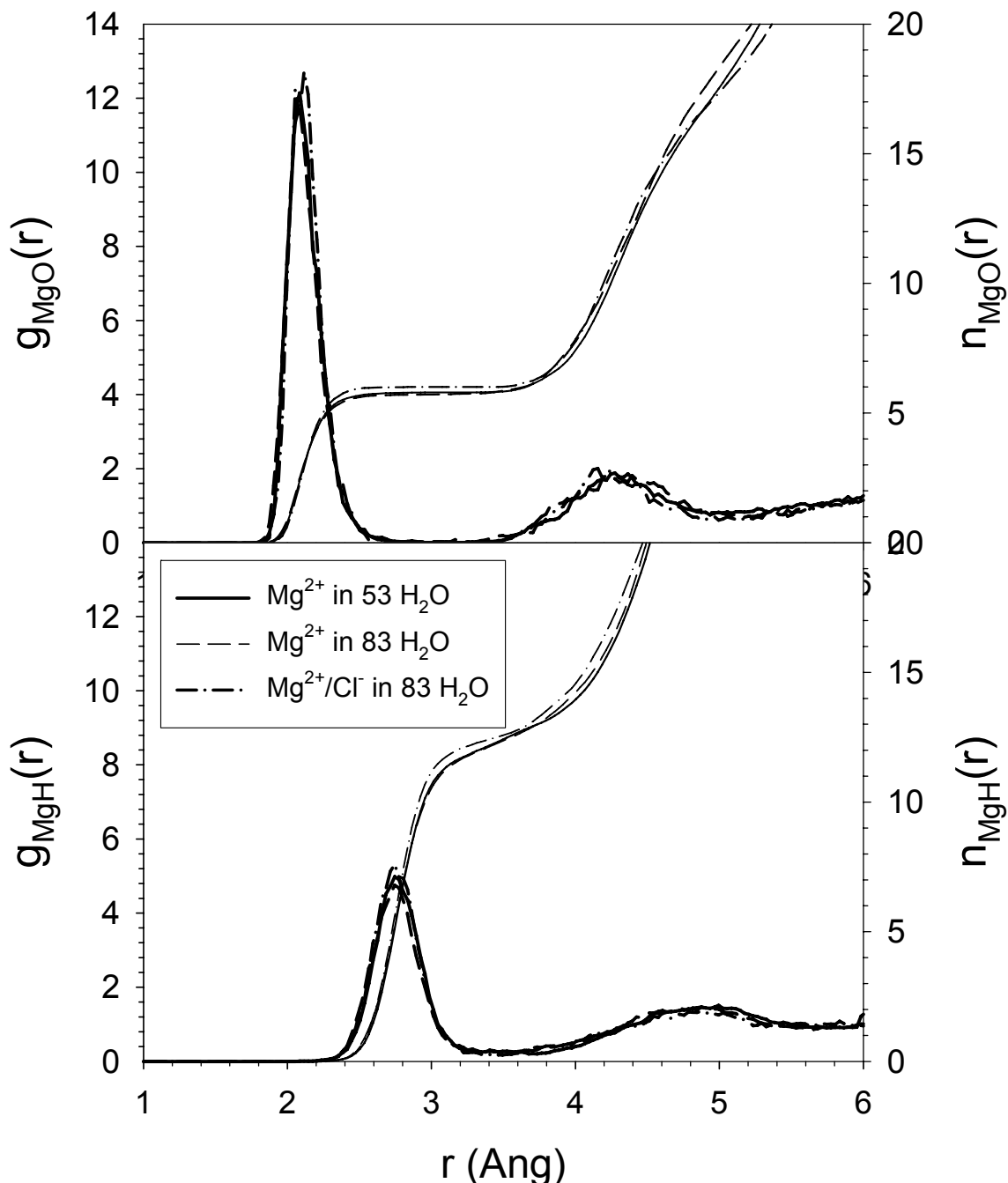


**Figure SI.5.** Mg–O and Mg–H radial distribution functions,  $g(r)$ , and running coordination number,  $n(r)$ , obtained from the CP-MD simulations of  $\text{Mg}^{2+}$  in 53 H<sub>2</sub>O,  $\text{Mg}^{2+}$  in 83 H<sub>2</sub>O and  $\text{Mg}^{2+}/\text{Cl}^-$  in 82 H<sub>2</sub>O.

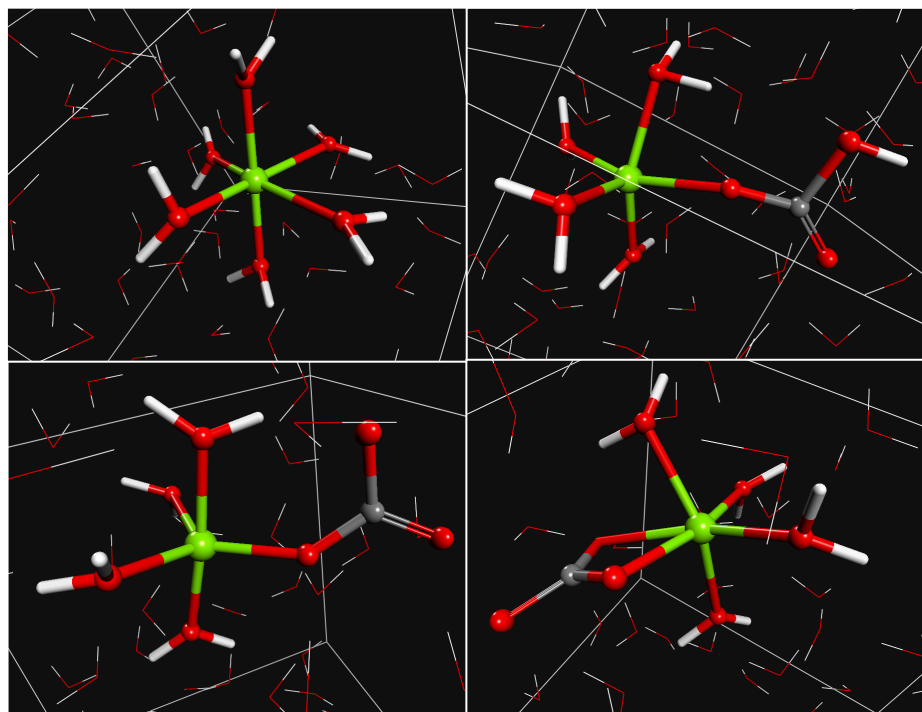


**Figure SI.6.** Representative snapshot taken from the CP-MD simulations showing the most stable species of the hydrated magnesium ion, and of the solvated magnesium bicarbonate and magnesium carbonate complexes.